IET Communications

Research Article

Performance comparison of two novel relay-assisted hybrid FSO/RF communication systems

ISSN 1751-8628
Received on 3rd June 2018
Revised 31st January 2019
Accepted on 21st March 2019
E-First on 14th May 2019
doi: 10.1049/iet-com.2018.5469
www.ietdl.org

Mohammad Ali Amirabadi[1] ✉, *Vahid Tabataba Vakili*[1]

[1]*School of Electrical Engineering, Iran University of Science and Technology, Tehran, Iran*

✉ *E-mail: m_amirabadi@elec.iust.ac.ir*

Abstract: In this study, two novel multi-hop relay-assisted hybrid FSO/RF communication systems are presented and compared. In these structures, RF and FSO links, at each hop, are parallel and send data simultaneously. This is the first time that in a multi-hop hybrid FSO/RF structure, detect and forward protocol is used. In the first structure, at each hop, received signals with a higher signal-to-noise ratio are selected. However, in the second structure, at each hop, received FSO and RF signals are separately detected and forwarded and selection is done only at the last hop. Considering FSO link in negative exponential atmospheric turbulence and RF link in Rayleigh fading, for the first time, closed-form expressions are derived for outage probability (P_{out}) and bit error rate of the proposed structures. MATLAB simulations are provided to verify derived expressions. Results indicate that the structure with the selection at each hop has better performance than the structure with a selection at the last hop.

1 Introduction

Free space optical (FSO) communication systems are considered as an appropriate alternative for traditional radio frequency (RF) communication systems. The FSO system has a large bandwidth compared with RF systems. In addition, because of a very narrow beam, FSO is highly secure and contains no interference. Besides these advantages, constraints such as high sensitivity to atmospheric turbulence and weather conditions severely limit FSO practical applications [1].

Various statistical distributions have been used to model atmospheric turbulence effects. Lognormal [2], Gamma–Gamma [3] and negative exponential [4] distributions are, respectively, used to model weak, moderate to strong and saturate atmospheric turbulence regimes.

The effects of atmospheric turbulences on FSO and RF links are not the same, in the sense that when atmospheric turbulences cause an outage in one of the FSO and RF links, the other link remains available. For example, severe rain does not affect the performance of the FSO link but degrades the performance of the RF link. Therefore a combination of FSO and RF links can significantly improve the performance and reliability of the system [5].

Hybrid FSO/RF systems are available in series [6, 7] and parallel [8, 9] structures. In a parallel structure, FSO and RF links are parallel and send data simultaneously [10] or by use of a switch [11]. In simultaneous data transmission, both FSO and RF links are always active, but in the switching method, FSO link is always active and RF link acts as a backup, i.e. when the received signal-to-noise ratio (SNR) comes down below a threshold level, RF link starts transmitting data. A series structure has lower power consumption but suffers from performance degradation due to frequent switches when atmospheric turbulence gets worse [12].

The so-called relay assisted hybrid FSO/RF systems improve the performance and capacity of the system. Different relay protocols have been studied for relay assisted systems; among them amplify and forward [13], due to its simplicity is mostly used. In this protocol, according to the existence or missing of channel state information (CSI), the received signal is amplified and forwarded by adaptive or fixed gain [14, 15]. Also, the case of outdated CSI is studied in [16]. Amplify and forward has high power consumption and amplifies noise. When CSI is missed, amplification gain should be adjusted according to the worst case scenario, therefore, it has power loss. It is better to use other protocols such as decode and forward [17] and detect and forward [18].

Works done about the so-called hybrid FSO/RF system can be divided into three main categories. The first category deals with single-hop parallel FSO/RF structure [19–21]. The second category investigates the performance of dual-hop structure [22–29]; some works used a direct backup link between source and destination [28]. The last category deals with multi-hop structure. The multi-hop structure was previously investigated in the FSO system [30–34], but in the FSO/RF system, it is considered as a new topic [35, 36]. In these works, a multi-hop hybrid FSO/RF link is implemented and outage probability of the system is investigated. To the best of the authors' knowledge, this is the first time a multi-hop relay-assisted hybrid FSO/RF system with parallel data transmission on each hop is being investigated at saturating atmospheric turbulence.

In this study, two novel models are presented for the multi-hop hybrid FSO/RF system. At each hop of the proposed structures, FSO and RF links are parallel and send data simultaneously. Detect and forward protocol is used. At each relay input, the first structure, which received a signal with a higher SNR, is selected. However, in the second structure, the received signal at each relay input is detected and forwarded separately, and selection is done only at the destination. To the best of the authors' knowledge, this is the first time that the detect and forward protocol is used for the multi-hop hybrid FSO/RF system. Also, it is the first time that bit error rate (BER) of a multi-hop hybrid FSO/RF is investigated. Considering the FSO link in negative exponential atmospheric turbulence and RF link in Rayleigh fading, for the first time, closed-form expressions are derived for BER and P_{out} of the proposed structures. Derived expressions are validated through MATLAB simulations. In proposed structures, a combination of FSO and RF links significantly increased link reliability and accessibility. In addition, multi-hop relaying reduces total power consumption and increases the capacity of the system. Also, detect and forward relaying used in this work has low cost and easy implementation.

The proposed structure could be useful in situations that the source and destination are far from each other, e.g. source and destination base stations located in two cities. The multi-hop structures are more useful in long-range links. Another implementation scenario is under bad atmospheric conditions; because a good communication idea under bad atmospheric

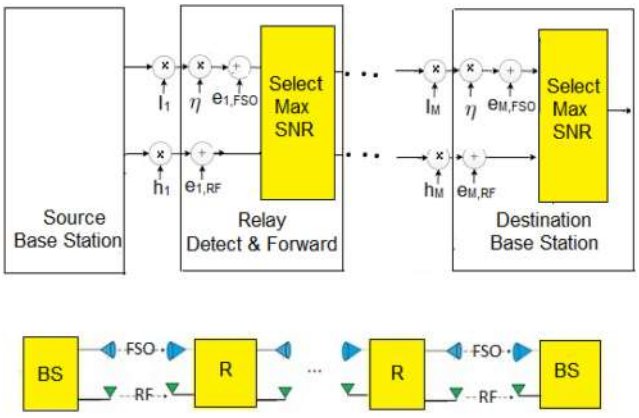

Fig. 1 *Structure with the selection at each hop*

conditions is reducing the link length; so, instead of a long link, use of multiple connected short links could really improve performance at such atmospheric scenarios.

The rest of this work is organised as follows. In Section 2, the system model, P_{out}, and BER of the structure with the selection at each hop are discussed. System model, P_{out}, and BER of the structure with the selection at the destination are expressed in Section 3. In Section 4, analytical and simulation results are compared and discussed. Section 5 is the conclusion of this work.

2 Structure with a selection at each hop

2.1 System model

The proposed multi-hop hybrid FSO/RF system is presented in Fig. 1. Assuming x as the generated signal at the source base station; two copies of this signal are transmitted through FSO and RF links. Between received FSO and RF signals at the first relay, the signal with higher SNR is detected, then two copies of this signal are forwarded through RF and FSO links. The same trend continues at each hop until reaching the destination base station.

Received FSO and RF signals at the ith ($i = 1, 2, \ldots, M$) relay are as follows:

$$y_{\text{FSO}.i} = \eta I_i d_{i-1} + e_{\text{FSO}.i}, \tag{1}$$

$$y_{\text{RF}.i} = h_i d_{i-1} + e_{\text{RF}.i}, \tag{2}$$

where d_{i-1} is the detected signal at the $(i-1)$th relay, h_i is the fading coefficient of the ith hop, I_i is the atmospheric turbulence intensity of the ith hop, $e_{\text{FSO}.i}$ is the additive white Gaussian noise (AWGN) with zero mean and σ^2_{FSO} variance at the input of the ith FSO receiver, $e_{\text{RF}.i}$, is the AWGN with zero mean and σ^2_{RF} variance at the input of the ith RF receiver, and η is the photodetector responsivity.

At each hop, between received FSO and RF signals, the signal with the highest SNR is selected for detection, i.e. $\gamma_i = \max(\gamma_{\text{FSO}.i} \cdot \gamma_{\text{RF}.i})$. Assuming independence of FSO and RF links, the cumulative distribution function (CDF) of γ_i becomes as follows:

$$F_{\gamma_i}(\gamma) = \Pr(\max(\gamma_{\text{FSO}.i} \cdot \gamma_{\text{RF}.i}) \le \gamma) = \Pr(\gamma_{\text{FSO}.i} \le \gamma \cdot \gamma_{\text{RF}.i} \le \gamma) = F_{\gamma_{\text{FSO}.i}}(\gamma) F_{\gamma_{\text{RF}.i}}(\gamma), \tag{3}$$

where $\gamma_{\text{FSO}.i}$ is the SNR at the input of the ith FSO receiver and $\gamma_{\text{RF}.i}$ is the SNR at the input of the ith RF receiver.

2.2 Outage probability

An outage occurs when the SNR comes below a threshold level, i.e. $\gamma \le \gamma_{\text{th}}$. Assuming that the detection done at each relay is independent of the detection done at other relays, P_{out} of the first proposed structure will be defined as follows [26]:

$$P_{\text{out}}(\gamma_{\text{th}}) = 1 - P_{\text{ava}}(\gamma_{\text{th}}) = 1 - \prod_{i=1}^{M} P_{\text{ava}.i}(\gamma_{\text{th}}) = 1 - \prod_{i=1}^{M} (1 - P_{\text{out}.i}(\gamma_{\text{th}})), \tag{4}$$

where $P_{\text{ava}} = 1 - P_{\text{out}}$ is the probability of link availability. So, given that $P_{\text{out}}(\gamma_{\text{th}}) = F_{\gamma}(\gamma_{\text{th}})$, and that FSO link atmospheric turbulence and RF link fading are independent and identically distributed, the above statement becomes equal to

$$P_{\text{out}}(\gamma_{\text{th}}) = 1 - (1 - F_{\gamma_i}(\gamma_{\text{th}}))^M = 1 - (1 - F_{\gamma_{\text{RF}.i}}(\gamma_{\text{th}}) F_{\gamma_{\text{FSO}.i}}(\gamma_{\text{th}}))^M. \tag{5}$$

Therefore, in order to obtain P_{out} of the first proposed structure, it is sufficient to calculate CDF of FSO and RF links, separately and then substitute them at (5).

The FSO link is described by the negative exponential atmospheric turbulence with $1/\lambda$ mean and $1/\lambda^2$ variance. The probability density function (pdf) of I_i is as follows:

$$f_{I_i}(I_i) = \lambda e^{-\lambda I_i}. \tag{6}$$

According to (1), instantaneous SNR at the ith FSO receiver is $\gamma_{\text{FSO}.i} = (\eta^2 I_i^2 / \sigma^2_{\text{FSO}}) = \bar{\gamma}_{\text{FSO}} I_i^2$, where $\bar{\gamma}_{\text{FSO}}$ is average SNR. Using [37] and (6), the pdf and CDF of $\gamma_{\text{FSO}.i}$ are equal to

$$f_{\gamma_{\text{FSO}.i}}(\gamma) = \frac{\lambda}{2\sqrt{\bar{\gamma}_{\text{FSO}}\gamma}} e^{-\lambda\sqrt{\gamma/\bar{\gamma}_{\text{FSO}}}}, \qquad F_{\gamma_{\text{FSO}.i}}(\gamma) = 1 - e^{-\lambda\sqrt{\gamma/\bar{\gamma}_{\text{FSO}}}}. \tag{7}$$

According to (2), the instantaneous SNR at the ith RF receiver is $\gamma_{\text{RF}.i} = (h_i^2/\sigma^2_{\text{RF}}) = \bar{\gamma}_{\text{RF}} h_i^2$, where $\bar{\gamma}_{\text{RF}}$ is the average SNR. The pdf and CDF of $\gamma_{\text{RF}.i}$ are equal to

$$f_{\gamma_{\text{RF}.i}}(\gamma) = \frac{1}{\bar{\gamma}_{\text{RF}}} e^{-(\gamma/\bar{\gamma}_{\text{RF}})}, \tag{8}$$

$$F_{\gamma_{\text{RF}.i}}(\gamma) = 1 - e^{-(\gamma/\bar{\gamma}_{\text{RF}})}. \tag{9}$$

Substituting (8) and (10) into (5), P_{out} of the proposed structure is as follows:

$$P_{\text{out}}(\gamma_{\text{th}}) = 1 - \left(1 - \left(1 - e^{-\lambda\sqrt{\gamma_{\text{th}}/\bar{\gamma}_{\text{FSO}}}}\right)\left(1 - e^{-(\gamma_{\text{th}}/\bar{\gamma}_{\text{RF}})}\right)\right)^M. \tag{10}$$

Substituting binomial expansion of

$$\left[1 - \left(1 - e^{-\lambda\sqrt{\gamma_{\text{th}}/\bar{\gamma}_{\text{FSO}}}}\right)\left(1 - e^{-(\gamma_{\text{th}}/\bar{\gamma}_{\text{RF}})}\right)\right]^M \quad \text{as} \quad \sum_{k=0}^{M} \binom{M}{k} (-1)^k \left(1 - e^{-\lambda\sqrt{\gamma_{\text{th}}/\bar{\gamma}_{\text{FSO}}}}\right)^k \left(1 - e^{-(\gamma_{\text{th}}/\bar{\gamma}_{\text{RF}})}\right)^k,$$

(11) becomes equal to

$$P_{\text{out}}(\gamma_{\text{th}}) = 1 - \sum_{k=0}^{M} \binom{M}{k} (-1)^k \left(1 - e^{-\lambda\sqrt{\gamma_{\text{th}}/\bar{\gamma}_{\text{FSO}}}}\right)^k \left(1 - e^{-(\gamma_{\text{th}}/\bar{\gamma}_{\text{RF}})}\right)^k. \tag{11}$$

Substituting binomial expansion of

$$\left(1 - e^{-(\gamma_{\text{th}}/\bar{\gamma}_{\text{RF}})}\right)^k \quad \text{and} \quad \left(1 - e^{-\lambda\sqrt{\gamma_{\text{th}}/\bar{\gamma}_{\text{FSO}}}}\right)^k,$$

Respectively, as

$$\sum_{v=0}^{k}\binom{k}{v}(-1)^{v}\mathrm{e}^{-(v\gamma_{\mathrm{th}}/\bar{\gamma}_{\mathrm{RF}})} \quad \text{and} \quad \sum_{u=0}^{k}\binom{k}{u}(-1)^{u}\mathrm{e}^{-\lambda u\sqrt{\gamma_{\mathrm{th}}/\bar{\gamma}_{\mathrm{FSO}}}},$$

P_{out} of the proposed structure becomes equal to

$$P_{\mathrm{out}}(\gamma_{\mathrm{th}}) = 1 - \sum_{k=0}^{M}\sum_{v=0}^{k}\sum_{u=0}^{k}\binom{M}{k}\binom{k}{v}\binom{k}{u}(-1)^{k+v+u}\mathrm{e}^{-(v\gamma_{\mathrm{th}}/\bar{\gamma}_{\mathrm{RF}})}\mathrm{e}^{-\lambda u\sqrt{\gamma_{\mathrm{th}}/\bar{\gamma}_{\mathrm{FSO}}}}. \tag{12}$$

P_{out} of the proposed structure is related exponentially to $1/\bar{\gamma}_{\mathrm{RF}}$ and $1/\sqrt{\bar{\gamma}_{\mathrm{FSO}}}$, therefore in order to improve the performance of the system, it is better to increase $\bar{\gamma}_{\mathrm{RF}}$, rather than $\bar{\gamma}_{\mathrm{FSO}}$. In the sense that increasing the transmitted power in RF link brings more improvement than that of FSO link.

2.3 Bit error rate

Though the performance of M-ary phase shift keying (MPSK) modulations is better than differential phase shift key (DPSK), but DPSK does not need the carrier phase estimation circuit and therefore, its receiver has less complexity. Given that $F_{\gamma}(\gamma) = P_{\mathrm{out}}(\gamma)$, BER for DPSK modulation is obtained from the following equation [38]:

$$P_{\mathrm{e}} = \frac{1}{2}\int_{0}^{\infty}\mathrm{e}^{-\gamma}F_{\gamma}(\gamma)\mathrm{d}\gamma = \frac{1}{2}\int_{0}^{\infty}\mathrm{e}^{-\gamma}P_{\mathrm{out}}(\gamma)\mathrm{d}\gamma\,. \tag{13}$$

Substituting (13) into (14), the BER of DPSK modulation of the proposed structure becomes equal to

$$P_{\mathrm{e}} = \frac{1}{2}\int_{0}^{\infty}\mathrm{e}^{-\gamma}\left(1 - \sum_{k=0}^{M}\sum_{v=0}^{k}\sum_{u=0}^{k}\binom{M}{k}\binom{k}{v}\binom{k}{u}(-1)^{k+v+u}\mathrm{e}^{-(v\gamma/\bar{\gamma}_{\mathrm{RF}})}\mathrm{e}^{-\lambda u\sqrt{\gamma/\bar{\gamma}_{\mathrm{FSO}}}}\right)\mathrm{d}\gamma\,. \tag{14}$$

By using (23), the Meijer-G equivalent of $\mathrm{e}^{-\lambda u\sqrt{\gamma/\bar{\gamma}_{\mathrm{FSO}}}}$ becomes as

$$\frac{1}{\sqrt{\pi}}G_{0,2}^{2,0}\left(\frac{\lambda^2u^2\gamma}{4\bar{\gamma}_{\mathrm{FSO}}}\middle|\begin{matrix}-\\0,\frac{1}{2}\end{matrix}\right).$$

By substituting this into (14) and using (24), the BER of DPSK modulation of the proposed structure becomes equal to

$$P_{\mathrm{e}} = \frac{1}{2}\left(1 - \sum_{k=0}^{M}\sum_{v=0}^{k}\sum_{u=0}^{k}\binom{M}{k}\binom{k}{v}\binom{k}{u} \times \frac{(-1)^{k+v+u}}{\sqrt{\pi}(1+(v/\bar{\gamma}_{RF}))}G_{1,2}^{2,1}\left(\frac{\lambda^2u^2}{4\bar{\gamma}_{\mathrm{FSO}}(1+(v/\bar{\gamma}_{\mathrm{RF}}))}\middle|\begin{matrix}0\\0,\frac{1}{2}\end{matrix}\right)\right). \tag{15}$$

3 Structure with a selection at the destination

3.1 System model

In Fig. 2, a relay-assisted hybrid FSO/RF communication system with M series hops is considered, in which FSO and RF links are parallel and send data simultaneously and separately. Assuming x as the generated signal at the source base station, two copies of the signal are transmitted through FSO and RF links. The received FSO and RF signals are then detected and forwarded separately.

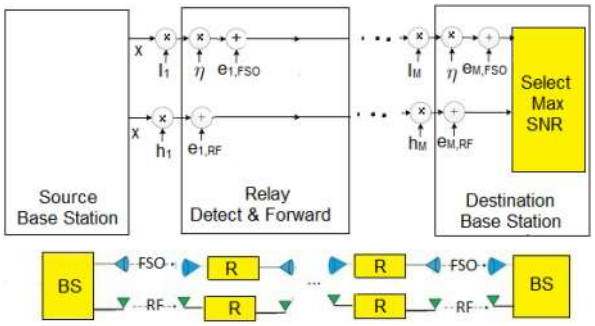

Fig. 2 *Structure with the selection at the destination*

This procedure continues until reaching the destination base station. At the destination, between received FSO and RF signals, one with higher SNR is used for detection.

The received FSO and RF signals at the ith relay are as follows:

$$y_{\mathrm{FSO}.i} = \eta I_i d_{\mathrm{FSO}.i-1} + e_{\mathrm{FSO}.i}, \tag{16}$$

$$y_{\mathrm{RF}.i} = h_i d_{\mathrm{RF}.i-1} + e_{\mathrm{RF}.i}, \tag{17}$$

where $d_{\mathrm{RF}.i-1}$ and $d_{\mathrm{FSO}.i-1}$ are, respectively, the detected FSO and RF signals at the $(i-1)$th relay.

3.2 Outage probability

Assuming independent FSO and RF links and independent detection at each relay, P_{out} of the second proposed structure is defined as follows: (see (18)) . Given that $P_{\mathrm{out}}(\gamma_{\mathrm{th}}) = F_{\gamma}(\gamma_{\mathrm{th}})$ and independent identically distributed FSO and RF links, (18) becomes equal to

$$P_{\mathrm{out}}(\gamma_{\mathrm{th}}) = (1-(1-F_{\gamma_{\mathrm{RF}.i}}(\gamma_{\mathrm{th}}))^{M})(1-(1-F_{\gamma_{\mathrm{FSO}.i}}(\gamma_{\mathrm{th}}))^{M})\,. \tag{19}$$

Substituting (8) and (10) into (20), P_{out} of the second proposed structure becomes equal to

$$P_{\mathrm{out}}(\gamma_{\mathrm{th}}) = 1 - \mathrm{e}^{-\lambda M\sqrt{\gamma_{\mathrm{th}}/\bar{\gamma}_{\mathrm{FSO}}}} - \mathrm{e}^{-(M\gamma_{\mathrm{th}}/\bar{\gamma}_{\mathrm{RF}})} + \mathrm{e}^{-(M\gamma_{\mathrm{th}}/\bar{\gamma}_{\mathrm{RF}})}\mathrm{e}^{-\lambda M\sqrt{\gamma_{\mathrm{th}}/\bar{\gamma}_{\mathrm{FSO}}}}. \tag{20}$$

3.3 Bit error rate

Substituting (20) into (14), and inserting Meijer-G equivalent of $\mathrm{e}^{-\lambda M\sqrt{\gamma/\bar{\gamma}_{\mathrm{FSO}}}}$ into it, the BER of DPSK modulation of the second proposed structure becomes as follows:

$$P_{\mathrm{e}} = \frac{1}{2}\int_{0}^{\infty}\mathrm{e}^{-\gamma}\left(1 - \frac{1}{\sqrt{\pi}}G_{0,2}^{2,0}\left(\frac{\lambda^2M^2\gamma}{4\bar{\gamma}_{\mathrm{FSO}}}\middle|\begin{matrix}0\\0,\frac{1}{2}\end{matrix}\right) - \mathrm{e}^{-(M\gamma/\bar{\gamma}_{\mathrm{RF}})} + \frac{1}{\sqrt{\pi}}\mathrm{e}^{-(M\gamma/\bar{\gamma}_{\mathrm{RF}})}G_{0,2}^{2,0}\left(\frac{\lambda^2M^2\gamma}{4\bar{\gamma}_{\mathrm{FSO}}}\middle|\begin{matrix}0\\0,\frac{1}{2}\end{matrix}\right)\right)\mathrm{d}\gamma\,. \tag{21}$$

Using (24), the BER of DPSK modulation of the second structure becomes equal to

$$P_{\mathrm{out}}(\gamma_{\mathrm{th}}) = P_{\mathrm{out}.\mathrm{FSO}}(\gamma_{\mathrm{th}})P_{\mathrm{out}.\mathrm{RF}}(\gamma_{\mathrm{th}}) = (1-P_{\mathrm{ava}.\mathrm{FSO}}(\gamma_{\mathrm{th}}))(1-P_{\mathrm{ava}.\mathrm{RF}}(\gamma_{\mathrm{th}})) = \left(1-\prod_{i=1}^{M}(1-P_{\mathrm{out}.\mathrm{RF}.i}(\gamma_{\mathrm{th}}))\right)\left(1-\prod_{i=1}^{M}(1-P_{\mathrm{out}.\mathrm{FSO}.i}(\gamma_{\mathrm{th}}))\right). \tag{18}$$

$$P_e = \frac{1}{2}\left(1 - \frac{1}{\sqrt{\pi}} G_{1,2}^{2,1}\left(\frac{\lambda^2 M^2}{4\bar{\gamma}_{FSO}}\middle|_{0,\frac{1}{2}}^{0}\right) - \frac{1}{1+(M/\bar{\gamma}_{RF})} + \frac{1}{\sqrt{\pi}}\frac{1}{1+(M/\bar{\gamma}_{RF})} G_{1,2}^{2,1}\left(\frac{\lambda^2 M^2}{4\bar{\gamma}_{FSO}(1+(M/\bar{\gamma}_{RF}))}\middle|_{0,\frac{1}{2}}^{0}\right)\right). \quad (22)$$

4 Comparison between analytical and simulation results

In this section, mathematical analysis and MATLAB simulation results are compared. FSO and RF links are described by negative exponential atmospheric turbulence and Rayleigh fading, respectively. Performances of the proposed structures are investigated at various variances of negative exponential atmospheric turbulence ($1/\lambda^2$) and various numbers of hops (M). FSO and RF links have equal average SNR ($\bar{\gamma}_{FSO} = \bar{\gamma}_{RF} = \gamma_{avg}$). γ_{th} is the outage threshold SNR.

In Fig. 3, the outage probability of the proposed structures is plotted in terms of average SNR for the various number of hops for negative exponential atmospheric turbulence with unit variance ($\lambda = 1$) and $\gamma_{th} = 10$ dB. As can be seen, the performance of the proposed structures degrades by increasing the number of hops. According to the definition of P_{out} and due to the use of series relaying structure, outage occurrence in the proposed structures is caused by the outage even in one hop, therefore adding the number of hops increases P_{out}. In fact, the multi-hop structure replaces high power consumption long-range link with some low power consumption short-range links.

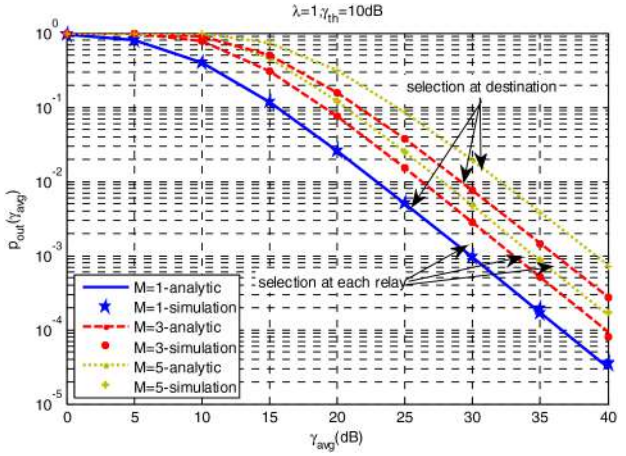

Fig. 3 *Outage probability of the proposed structures in terms of average SNR for various number of hops for negative exponential atmospheric turbulence with unit variance ($\lambda = 1$) and $\gamma_{th} = 10$ dB*

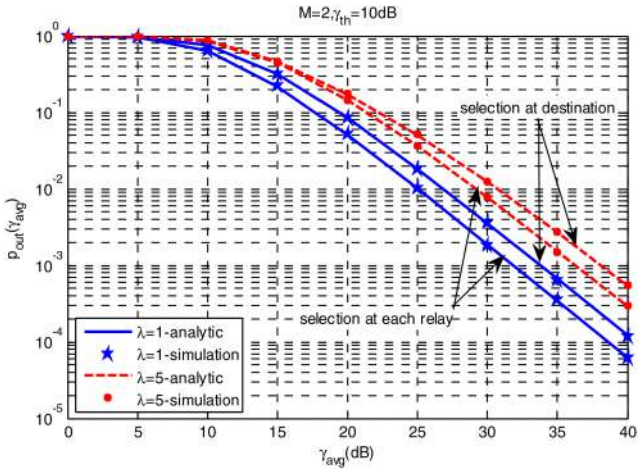

Fig. 4 *Outage probability of the proposed structures in terms of average SNR for various variances of negative exponential atmospheric turbulence when $M = 2$ and $\gamma_{th} = 10$ dB*

As can be seen, the structure with selection at each hop has better performance than the other structure, because in the structure with selection at each hop, between the two received FSO and RF signals, the one with higher SNR is used for detection at each hop but at the structure with selection at the destination, each of the received FSO and RF signals are detected and forwarded separately. Therefore P_{out} of the structure with a selection at each hop is less than the other structure. It can be seen that at a different target P_{out}, in both proposed structures, γ_{avg} difference between the cases of $M = 1$ and $M = 3$ is more than the cases of $M = 3$ and 5. It is expected that when $M \to \infty$, system performance reaches a steady state and increasing number of hops does not degrade it any more.

In Fig. 4, the outage probability of the proposed structures is plotted in terms of average SNR for various variances of negative exponential atmospheric turbulence when $M = 2$ and $\gamma_{th} = 10$ dB. As can be seen, the structure with a selection at each relay has better performance at various variances of negative exponential atmospheric turbulence. It can be seen that at high intensity of negative exponential atmospheric turbulence ($\lambda = 5$), and different target P_{out}, there is a slight γ_{avg} difference between the proposed structures. In each of the proposed structures, when $P_{out} \leq 10^{-2}$, γ_{avg} difference between system performance at various variances of negative exponential atmospheric turbulence is fixed. This is a kind of stability, in the sense that addition of a constant fraction of consuming power, maintains the performance of the system and there is no need to change this fraction at different situations. This feature eliminates the need for an adaptive processor that changes additional power fraction according to atmospheric turbulences. Therefore, the proposed structures have less complexity, power consumption, and processing delay. Supplying the required power is the major issue in the links with a saturate atmospheric turbulence regime, hence the proposed structures, due to their properties, are particularly suitable for such links.

In Fig. 5, the BER of the proposed structures is plotted in terms of average SNR for a various number of hops for negative exponential atmospheric turbulence with unit variance ($\lambda = 1$). As can be seen, at different target P_{out}, γ_{avg} difference between cases of $M = 2$ and 1 in the structure with selection at each hop is about 2 dB and in the structure with selection at the destination is about 4.5 dB, meaning that the structure with selection at the destination consumes about twice (~ 3 dB) more power to maintain theperformance. It is also observed that the performance difference between the proposed structures increases by adding the number of hops. For example, at $P_{out} = 10^{-3}$, $gamma_{avg}$ difference between the proposed structures in cases of $M = 1, 2, \text{and} 3$ are, respectively, about 0, 2, and 3 dB. Since the structure with the selection at the destination makes only one decision, but the other structure makes a decision every hop, also detection of each relay is independent of other relays. Therefore, an increasing number of hops increases the number of total decisions, thereby increases the number of total errors.

In Fig. 6, the BER of the proposed structures is plotted in terms of average SNR for various variances of negative exponential atmospheric turbulence when $M = 2$. As can be seen, at low γ_{avg}, the difference between performances of the proposed structures at various atmospheric turbulence variances is not so much, but at high γ_{avg} this difference increases. Since at low γ_{avg}, the noise effect is dominant, i.e. performance degradation is mostly due to the noise effect, but by an increase of γ_{avg}, the effect of atmospheric turbulence overcomes the noise effect. At different target P_e, γ_{avg} difference between the proposed structures at various atmospheric turbulence variances is the same. When the number of hops is constant, in fact, the number of made decisions is constant, thereby performance difference between proposed structures, which depends on the number of made decisions, is constant and does not change by a change in atmospheric turbulence variance.

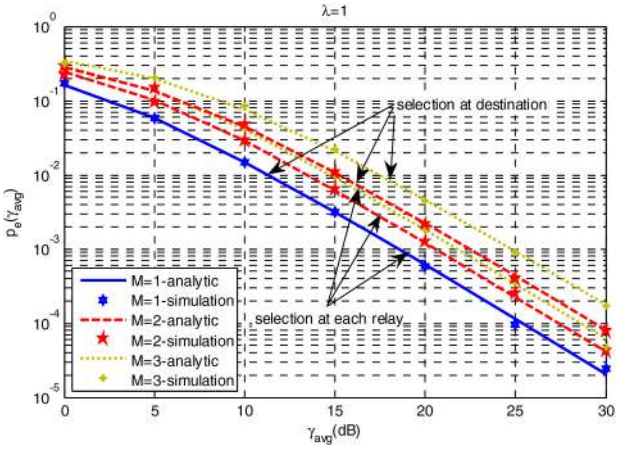

Fig. 5 *BER of the proposed structures in terms of average SNR for various number of hops, for negative exponential atmospheric turbulence with unit variance ($\lambda = 1$)*

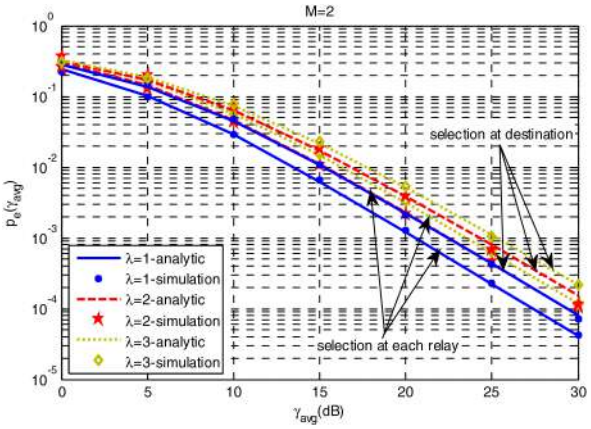

Fig. 6 *BER of the proposed structures in terms of average SNR for various variances of negative exponential atmospheric turbulence when M = 2*

5 Conclusion

In this study, two novel models are presented for a multi-hop hybrid FSO/RF communication system. In both structures, a series multi-hop relay assisted hybrid FSO/RF link, connects source and destination base stations. It is the first time that in a multi-hop relay assisted hybrid FSO/RF structure, a detect and forward relaying scheme is used. One of the proposed structures makes decisions at each hop, but the other makes a decision only at the last hop. Considering FSO link in negative exponential atmospheric turbulence and RF link in Rayleigh fading, for the first time, closed-form expressions are derived for BER and P_{out} of the proposed structures and the derived expressions are verified through MATLAB simulations. It is noteworthy to mention that this is the first time that BER of a multi-hop hybrid FSO/RF structure is being investigated.

The performance of the proposed structures is compared and investigated at various numbers of hops and different variances of negative exponential atmospheric turbulence. It is observed that an increasing number of hops degrade the performance of both structures. However, overall, the performance of the first structure is better than the second one, because in the first structure, each relay selects signal with higher SNR for detection but in the second structure, each of the FSO and RF signals is detected and forwarded separately.

Results indicate that at different target P_{out}, a structure with the selection at the destination consumes about two times (~ 3 dB) more power than the first structure to maintain performance. At low γ_{avg}, the difference between performances of the proposed structures at various atmospheric turbulence variances is negligible, therefore the proposed structures are almost independent of atmospheric turbulences and do not need an adaptive processor or consuming much more power to maintain performance, thus they have low complexity, power consumption, and processing delay. The proposed structures, due to their properties, are particularly suitable for saturating atmospheric turbulence and long-range links, where supplying the required power is the major problem.

6 References

[1] Jamali, V., Michalopoulos, D. S., Uysal, M., *et al.*: 'Resource allocation for mixed RF and hybrid RF/ FSO relay', 2015

[2] Lopez-Martinez, F. J., Gomez, G., Garrido-Balsells, J. M.: 'Physical-Layer security in free space optical communications', *IEEE Photonics J.*, 2015, **7**, pp. 1–14

[3] Kaushal, H., Jain, V.K., Ka, S.: '*Free space optical communication*' (Springer, India, 2017), p. 60

[4] Amirabadi, M. A., Vakili, V. T.: 'On the performance of a relay-assisted multi-hop asymmetric FSO/RF communication system over negative exponential atmospheric turbulence with the effect of pointing error'. arXiv preprint arXiv:1808.10277, 2018

[5] Mai, V. V., Pham, A. T.: 'Designs for multi-rate hybrid adaptive FSO/RF systems over fading channel'. Globecom Workshops, Austin, TX, USA, 2014

[6] Zhang, J., Dai, L., Zhang, Y., *et al.*: 'Unified performance analysis of mixed radio frequency/free-space optical dual-hop transmission systems', *J. Lightwave Technol.*, 2015, **33**, pp. 2286–2293

[7] Jing, Z., Shang-hong, Z., Wei-hu, Z., *et al.*: 'Performance analysis for mixed FSO/RF Nakagami-m and exponentiated Weibull dual-hop airborne systems', *Opt. Commun.*, 2017, **392**, pp. 294–299

[8] Kumar, K., Borah, D. K.: 'Hybrid FSO/RF symbol mappings: merging high speed FSO with low speed RF through BICM-ID'. IEEE Global Communications Conf., Anaheim, CA, USA, 2012

[9] Abdulhussein, A., Oka, A., Nguyen, T. T., *et al.*: 'Rateless coding for hybrid free-space optical and radio-frequency communication', *IEEE Trans. Wirel. Commun.*, 2010, **9**, pp. 907–913

[10] Rakia, T., Yang, H.C., Gebali, F., *et al.*: 'Power adaptation based on truncated channel inversion for hybrid FSO/RF transmission with adaptive combining', *IEEE Photonics J.*, 2015, **7**, pp. 1–12

[11] Rakia, T., Yang, H. C., Alouini, M. S., *et al.*: 'Outage analysis of practical FSO/RF hybrid system With adaptive combining', *IEEE Commun. Lett.*, 2015, **19**, pp. 1366–1369

[12] Mai, V. V., Pham, A. T.: 'Adaptive multi-rate designs and analysis for hybrid FSO/RF systems over fading channel', *IEICE Trans. Commun.*, 2015, **e98-B**, pp. 1660–1671

[13] Zedini, E., Soury, H., Alouini, M. S.: 'Dual-hop FSO transmission systems over gamma–gamma turbulence with pointing errors', *IEEE Trans. Wirel. Commun.*, 2017, **16**, pp. 784–796

[14] Kumar, N., Bhatia, V.: 'Performance analysis of amplify-and-forward cooperative networks with best-relay selection over Weibull channels fading', *Wirel. Pers. Commun.*, 2015, **85**, pp. 641–653

[15] Zedini, E., Soury, H., Alouini, M. S.: 'On the analysis of dual-hop mixed performance FSO/RF system', *IEEE Trans. Wirel. Commun.*, 2016, **15**, pp. 3679–3689

[16] Djordjevic, G., Petkovic, M., Cvetkovic, A., *et al.*: 'Mixed RF/FSO relaying with outdated channel state information', *IEEE J. Sel. Areas Commun.*, 2015, **PP**, pp. 1935–1948

[17] Varshney, N., Puri, P.: 'Performance analysis of decode-and-forward MIMO-based mixed RF/ FSO source mobility and cooperative systems with imperfect CSI', *J. Lightwave Technol.*, 2017, **35**, pp. 2070–2077

[18] Saidi, H., Tourki, K., Hamdi, N.: 'Performance analysis of PSK modulation in DF dual-hop hybrid RF/FSO system over gamma–gamma channel'. Int. Symp. on Signal, Image, Video and Communications (ISIVC), Tunis, Tunisia, 2016

[19] Khan, M. N., Jamil, M.: 'Adaptive hybrid free space optical/radio frequency communication system', *Telecommun. Syst.*, 2017, **65**, (1), pp. 117–126

[20] Chen, L., Wang, W., Zhang, C.: 'Multiuser diversity over parallel and hybrid FSO/RF links and its performance analysis', *IEEE Photonics J.*, 2016, **8**, pp. 1–9
[21] Amirabadi, M. A., Vakili, V. T.: 'A novel hybrid FSO/RF communication system with receive diversity'. arXiv preprint arXiv:1802.07348, 2018
[22] Trinh, P. V., Thang, T. C., Pham, A. T.: 'Mixed mmWave RF/FSO relaying systems over generalized fading channels with pointing errors', *IEEE Photonics J.*, 2017, **9**, (1), pp. 1–14
[23] Varshney, N., Puri, P.: 'Performance analysis of decode-and-forward-based mixed MIMO-RF/FSO cooperative systems with source mobility and imperfect CSI', *J. Lightwave Technol.*, 2017, **35**, (11), pp. 2070–2077
[24] Anees, S., Bhatnagar, M.: 'Performance of an amplify-and-forward dual-hop asymmetric RF–FSO communication system', *IEEE/OSA J. Opt. Commun. Networking*, 2015, **7**, pp. 124–135
[25] Amirabadi, M. A., Vakili, V. T.: 'Performance analysis of a novel hybrid FSO/RF communication system'. arXiv preprint arXiv:1802.07160, 2018
[26] Amirabadi, M. A., Vakili, V. T.: 'Performance analysis of hybrid FSO/RF communication systems with Alamouti coding or antenna selection'. arXiv preprint arXiv:1802.07286, 2018
[27] Amirabadi, M. A., Vakili, V. T.: 'On the performance of a CSI assisted dual-Hop asymmetric FSO/RF communication system over gamma-gamma atmospheric turbulence considering the effect of pointing error'. Int. Congress on Science and Engineering, Hamburg, Germany, 2018
[28] Bag, B., Das, A., Ansari, I. S., *et al.*: 'Performance analysis of hybrid FSO systems using FSO/RF-FSO link adaptation', *IEEE Photonics J.*, 2018, **10**, (3), pp. 1–17
[29] Bag, B., Das, A., Chandra, A., *et al.*: 'Capacity analysis for Rayleigh/gamma-gamma mixed RF/FSO link with fixed-gain AF relay', *IEICE Trans. Commun.*, 2017, **100**, (10), pp. 1747–1757
[30] Tsiftsis, T. A., Sandalidis, H. G., Karagiannidis, G. K., *et al.*: 'Multihop free-space optical communications over strong turbulence channels'. IEEE Int. Conf. on Communications, 2006 (ICC'06), Istanbul, Turkey, 2006, pp. 2755–2759
[31] Wang, P., Cao, T., Guo, L., *et al.*: 'Performance analysis of multihop parallel free-space optical systems over exponentiated Weibull fading channels', *IEEE Photonics J.*, 2015, **7**, (1), pp. 1–17
[32] Kashani, M. A., Uysal, M.: 'Outage performance of FSO multi-hop parallel relaying'. 2012 20th IEEE Signal Processing and Communications Applications Conf. (SIU), Mugla, Turkey, 2012, pp. 1–4
[33] Kashani, M. A., Uysal, M.: 'Outage performance and diversity gain analysis of free-space optical multi-hop parallel relaying', *J. Opt. Commun. Netw.*, 2013, **5**, (8), pp. 901–909
[34] Farhadi, G., Beaulieu, N. C.: 'Capacity of amplify-and-forward multi-hop relaying systems under adaptive transmission', *IEEE Trans. Commun.*, 2010, **58**, (3), pp. 758–763
[35] Makki, B., Svensson, T., Brandt-Pearce, M., *et al.*: 'Performance analysis of RF FSO multi-hop networks'. IEEE Wireless Communications and Networking Conf., San Francisco, CA, USA, 2017
[36] Kazemi, H., Uysal, M., Touati, F., *et al.*: 'Outage performance of multi-hop hybrid FSO/RF communication systems'. 4th Int. Workshop on Optical Wireless Communications, Istanbul, Turkey, 2015
[37] Papoulis, A., Pillai, S. U.: '*Probability, random variables, and stochastic presses*' (McGraw-Hill, New York, USA, 2002, 4th edn.), p. 132
[38] Kong, L., Xu, W., Hanzo, L., *et al.*: 'Performance of a free-space-optical relay-assisted hybrid RF/FSO system in generalized M-distributed channels', *IEEE Photon. J.*, 2015, **7**
[39] Wolfram, The Wolfram functions site, http://functions.wolfram.com./HypergeometricFunctions/MeijerG/, Accessed 2017

7 Appendix: the Meijer-G statement

In mathematics, the G-function was introduced by Cornelis Simon Meijer (1936) as a very general function intended to include most of the known special functions as particular cases. In the modern definition, the majority of the established special functions can be represented in terms of the Meijer-G function, e.g. the exponential functions could be stated in terms of the Meijer G-function as [39, Eq. 07.34.03.1081.01]:

$$G_{0,m}^{m,0}\left(z\middle|\begin{matrix}-\\ b\,.\,b+\frac{1}{m},b+\frac{2}{m},\ldots,b+\frac{m-1}{m}\end{matrix}\right)=\frac{(2\pi)^{(m-1)/2}}{\sqrt{m}}z^{b}\mathrm{e}^{-mz^{1/m}};\quad m\in N^{+}. \tag{23}$$

The main usage of the Meijer-G function is to solve complicated integrals. Simply, by substituting the Meijer-G function, most of the complicated integrals could be solved. One of the mostly used formulae for solving integrals of Meijer-G functions is as follows [39, Eq. 07.34.21.0088.01]: (see (24)) , where

$$c^{*}=m+n-\frac{p+q}{2}, \tag{25}$$

$$\mu=\sum_{j=1}^{q}b_j-\sum_{j=1}^{p}a_j+\frac{p-q}{2}+1. \tag{26}$$

$$\int_0^{\infty}\tau^{\alpha-1}\mathrm{e}^{-\sigma\tau}G_{p,q}^{m,n}\left(\omega\tau^{\frac{l}{k}}\middle|\begin{matrix}a_1,\ldots,a_n,a_{n+1},\ldots,a_p\\ b_1,\ldots,b_m,b_{m+1},\ldots,b_q\end{matrix}\right)\mathrm{d}\tau=\frac{k^{\mu}l^{\alpha-(1/2)}\sigma^{-\alpha}}{(2\pi)^{(l-1/2)+(k-1)c^{*}}}\times G_{kp+1,kq}^{km,kn+1}\left(\frac{\omega^{k}l^{l}}{\sigma^{l}k^{k(q-p)}}\middle|\begin{matrix}\frac{1-\alpha}{l},\ldots,\frac{l-\alpha}{l},\frac{a_1}{k},\ldots,\frac{k+a_1-1}{k},\ldots,\frac{a_n}{k},\ldots,\frac{k+a_n-1}{k},\ldots,\frac{a_p}{k},\ldots,\frac{k+a_p-1}{k},\\ \frac{b_1}{k},\ldots,\frac{k+b_1-1}{k},\ldots,\frac{b_m}{k},\ldots,\frac{k+b_m-1}{k},\ldots,\frac{b_q}{k},\ldots,\frac{k+b_q-1}{k}\end{matrix}\right);\quad k\in k\in N^{+}\Lambda l\in N^{+}, \tag{24}$$